DOI: 10.1002/marc.((insert number)) ((or ppap., mabi., macp., mame., mren., mats.))

Communication

Termination mechanism of the radical polymerization of acrylates

Yasuyuki Nakamura, Richmond Lee, Michelle Coote,* and Shigeru Yamago*

_____

Dr. Y. Nakamura, Prof. Dr. S. Yamago
Institute for Chemical Research, Kyoto University
Gokayo, Uji, Kyoto 611-0011 (Japan)
E-mail: yamago@scl.kyoto-u.ac.jp

R. Lee, Prof. Dr. M. Coote
ARC Centre of Excellence for Electromaterials Science, Research School of Chemistry, Australian National University
Canberra ACT 2601 (Australia)
E-mail: michelle.coote@anu.edu.au

_____

The termination mechanism of the radical polymerization of acrylates, namely the selectivity of disproportionation (Disp) and combination (Comb) between polymer end radicals, is unambiguously determined by the reaction of polyacrylate end radicals generated from corresponding “living” organotellurium ω-end polymer. While textbooks describe the occurrence of Comb, the reaction at 25 °C exclusively gives the Disp products. Ab initio molecular dynamics suggests that the products form by two pathways: the direct disproportionation reaction and a novel stepwise process that involves the initial formation of the C-O coupling product followed by intramolecular rearrangement. The termination at high temperature and low radical concentration increases the contribution of back-biting reaction giving mid-chain radicals, and complex reaction pathways of the mid-chain radicals are clarified for the first time.

FIGURE FOR ToC_ABSTRACT

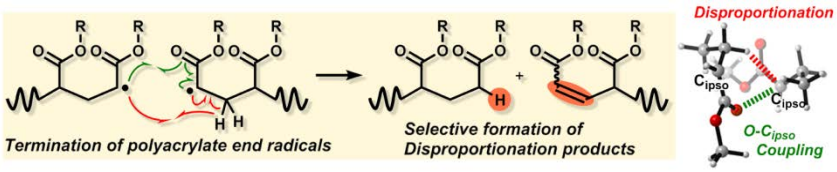
Termination of polyacrylate end radicals
Selective formation of
Disproportionation products
Disproportionation
C ipso
C ipso
O-C ipso
Coupling

1. Introduction

While radical polymerization is the most important technique in industry to produce polymer materials, the termination mechanism, e.g., contribution of disproportionation (Disp) and combination (Comb) of polymer-end radicals, is not yet fully understood.[1] Because the selectivity of Disp and Comb affects the molecular weight and chain end structure of the polymer products and further to properties of the polymer materials, the understanding of the selectivity is essential in polymer synthesis and design of polymer materials.

There have been numerous reports to elucidate the selectivity of the termination of acrylates, which is one of the most important monomers in polymer chemistry, but the conclusion is totally controversial.[2] For example, Bamford reported the termination mechanism in methyl acrylate (MA) polymerization exclusively Disp by viscosity analysis in 1955,[2a] while Ayrey reported the occurrence of exclusive Comb by the end group analysis in MA polymerization initiated by ^{14}C-labeled azo initiator in 1977.[2d] Although no clear conclusion of the mechanism in acrylate polymerization has been obtained, Comb is widely accepted to be the major mechanism as described in some textbooks[1] probably based on the general understanding of the termination mechanism of styrene (mono substituted vinyl monomer) and methyl methacrylate (α-methyl vinyl monomer), which undergo mainly by Comb and Disp, respectively. More recently, Barner-Kowollik elucidated the termination mechanism of photo-initiated polymerization of MA by mass spectroscopy and concluded that Comb is the major mechanism.[2e] However, the conclusion is not fully supported experimentally because the analyzed mass range was quite limited and the effect of the primary radicals generated from the initiators was not taken into account.

We have recently developed a new and highly efficient method to clarify the termination mechanism based on the product analysis.[3] Polymer-end radicals with controlled number average molecular weight (M_n) and low polydispersity are generated from the corresponding "living" polymer having the organotellurium-end group and are reacted each other giving

Disp and/or Comb products. Analysis of molecular weights and end-group structure unambiguously clarifies the contribution of Disp and Comb, because M_n of the Comb product is twice as that of the Disp products, and the Disp products shoud consist of a 1:1 mixture of end-hydrogenated and end-dehydrogenated products. Application of this method for the termination of methyl methacrylate and styrene polymerizations, namely, the reactions of poly(methyl methacrylate) and polystyrene end radicals, definitively clarified the differing selectivity of the termination reaction in these two systems.

In this report, we have applied this method to clarify the termination mechanism in acrylate polymerization starting from poly(methyl acrylate) (PMA) **1a** prepared by organotellurium-mediated radical polymerization (Scheme 1).[4] Surprisingly, we found that the reaction of the acrylate-end radicals **2** exclusively or predominantly gave Disp products **3** and **4** at low to ambient temperature. The result is different from the description in textbooks. Theoretical calculations suggest that Disp products **3** and **4** derive from two pathways, namely, the standard direct disproportionation reaction and a novel stepwise process involving initial formation of the C-O coupling product followed by intramolecular rearrangement. This stepwise pathway for the formation of the Disp products has not previously been reported.

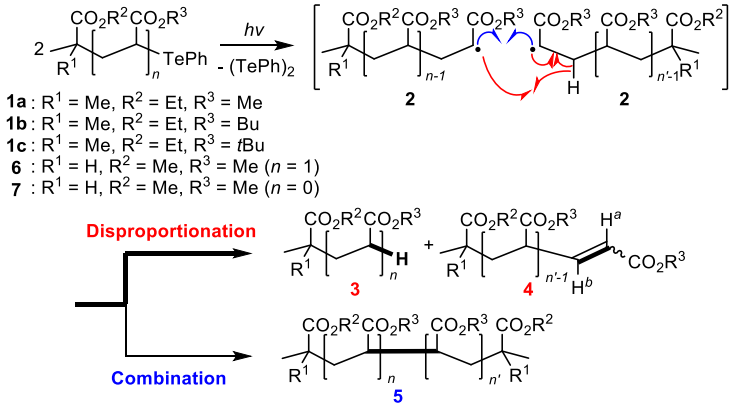

Scheme 1. Termination of polyacrylate-end radicals.

In addition, the effects of reaction conditions, such as reaction temperature, concentration, and molecular weight were also examined. It was found that the back-biting reaction, forming

mid-chain radicals, significantly increased at high temperature and low radical concentration. Furthermore, the complex reaction pathways of the mid-chain radicals were clearly identified for the first time.

2. Experimental Section

2.1. General

All reaction conditions dealing with oxygen sensitive compounds were carried out in a dry Pyrex reaction vessel under nitrogen atmosphere. A 500 W high pressure mercury lamp with combination of a cutoff filter (Asahi Techno Glass), and 6 W white LED with combination of neutral density filter (Sigma Koki) were used as light sources. In the photoirradiation experiment, the distance between light source and reaction vessel was set to be 10 cm.

2.2. Material

Unless otherwise noted, chemicals obtained from commercial suppliers were used as received. Benzene, trifluoromethylbenzene and dichloromethane were distilled over CaH_2. Methyl acrylate (MA) was washed with 5 % aqueous NaOH solution and were distilled over CaH_2. Ethyl 2-(phenylltellanyl)isobutyrate[1] were prepared as reported.

2.3. Characterization

^1H NMR (400 MHz) and ^{13}C NMR (100 MHz) spectra were measured for a $CDCl_3$, C_6D_6 or toluene-d_8 solution of a sample and are reported in ppm (δ) from internal tetramethylsilane or from solvent peak. Gel permeation chromatography (GPC) was performed on a machine equipped with polystyrene (PSt) mixed gel columns (two linearly connected Shodex LF-804) at 40 °C using RI and UV detectors. THF or $CHCl_3$ were used as eluent for GPC. The GPC was calibrated with PMMA standards. High resolution mass spectra (HRMS) were obtained under fast atom-bombardment (FAB) conditions. Matrix-assisted laser desorption/ionization time-of-flight mass spectrometry (MALDI-TOF-MS) spectra were recorded using positive reflector mode

with 20 kV acceleration voltages. Samples were prepared by mixing a THF solution of a polymer (10 mg/mL), dithranol (10 mg/mL), and sodium trifluoroacetate (5 mg/mL) in a ratio of 1:1:1.

2.4. Peak resolution analysis of GPC data

The GPC trace after the reaction was divided into two components by peak resolution method reported by Fukuda et al.[2] Typically M_n of one component was corresponding to that of starting living polymer, and that of the other was almost double of the starting polymer. These two components are respectively corresponding to disproportionation and combination products, and thus the area ratio of these components gives the ratio of occurrence of disproportionation and combination. A dead polymer terminated during the preparation of starting living polymer is included in the low molecular weight component, this amount is subtracted from the weight of the low molecular weight component upon the calculation of disproportionation and combination.

2.5. Computational method

Ab initio molecular dynamics and density functional theory (DFT) calculations were carried with Gaussian 09 computational suite[3]. Molecular dynamics simulation was carried in Atom-centered Density Matrix Propagation (ADMP) formalism[4-6] and DFT optimization of equilibrium structures at M11[7]/6-31+G(d,p)[8, 9] level of theory.

Molecular dynamics trajectories were propagated based on equilibrium structure of a caged triplet terminal radical fragment complex, ^{3}**2a-cpx**. This geometry where the SOMOs of the fragments are orthogonal allows optimal mixing of the triplet and singlet electronic states, thereby intersystem crossing to occur. Initial nuclear kinetic energies were set with the equation 1.5(N-1)*k*T*1e6/(J to au) to simulate the thermal conditions at 25°C and 120°C. All trajectories were run independently with the I/O option 1/44=-1 invoked to generate a random seed such that each runs were unique due to randomized atomic velocities. All runs ended about 200 fs via either the disproportionation or combination termination process.

2.6. Living poly(methyl acrylate) bearing phenyl tellanyl ω-end group (1a)

A solution of MA (2.50 mL, 27.6 mmol) and ethyl 2-(phenylltellanyl)isobutyrate (139 μL, 0.61 mmol) were irradiated using LED lamp equipped with neutral density filter of 50% transmittance at 40 °C for 30 min under a nitrogen atmosphere. A small portion of the reaction mixture was removed, and the conversion of the monomer (59%) was determined by ^{1}H NMR spectroscopy. The reaction mixture was placed under vacuum to remove remaining monomer to give living poly(methyl acrylate) bearing phenyl tellanyl ω-end group (1.41 g, 55% yield). M_n (3200) and M_w/M_n (1.20) were determined by using GPC. Living poly(butyl acrylate) and poly(*t*-butyl acrylate) were synthesized in the similar procedure.

2.7. Termination reaction of poly(methyl acrylate) end radicals

A solution of PMA bearing phenyltellanyl ω-chain end groups (M_n = 3200–34800, $M_w/M_n \leq 1.2$) was prepared in the desired solvent in a Pyrex glass tube under nitrogen atmosphere. The solution was photoirradiated with a 500 W high pressure Hg lamp through a 390 nm cut-off filterh. After the completion of the reaction (as monitored by ^{1}H NMR for the quantitative formation of diphenyl ditelluride), the reaction mixture was analyzed by ^{1}H NMR, GPC calibrated against PMMA standards with THF or $CHCl_3$ as an eluent, and finally, by MALDI-TOF MS.

2.8. Methyl 2-(phenyltellanyl)propionate (7)

Phenyl lithium (35 mL, 0.97 M in cyclohexane and diethyl ether, 34.1 mmol) was added slowly to a suspension of tellurium powder (4.8 g, 37.5 mmol) in THF (35 mL) at 0 °C under nitrogen atmosphere, and the resulting solution was stirred at rt for 40 min. To this solution was added methyl 2-bromopropionate (3.78 mL, 34.1 mmol) at 0 °C, and the mixture was stirred at rt for 4 h. Degassed water was added, and the aqueous phase was separated under a nitrogen atmosphere. The remaining organic phase was washed with degassed saturated aqueous NH_4Cl solution, dried over $MgSO_4$ and filtered under nitrogen atmosphere. The solvent was removed under reduced pressure followed by distillation (90-95 °C/0.6 mmHg) to give methyl 2-phenyltellanylpropionate (4.18 g, 42%) as orange oil. ^{1}H NMR ($CDCl_3$): δ 1.68 (d, J = 7.1 Hz, 3H, CH_3), 3.60 (s, 3H, OCH_3), 3.95 (q, J = 7.1 Hz, 1H, CH), 7.25 (t, J = 7.4 Hz, 2H, Ph), 7.37 (t, J = 6.9 Hz, 1H, Ph),. 7.85 (d, J = 7.4 Hz, 2H, Ph). ^{13}C NMR ($CDCl_3$): δ 17.4, 19.2, 51.9, 111.5, 128.9, 129.1, 140.9, 175.8. HRMS (FAB) *m*/*z*: found 293.9900; calcd for $C_{10}H_{12}O_2Te$ $[M]^+$, 293.9900.

2.9. Dimethyl 2-methyl-4-(phenyltellanyl)pentanodioate (6)

A solution of methyl 2-phenyltellanylpropionate (0.40 g, 1.37 mmol) and methyl acrylate (0.124 mL, 1.37 mmol) in trifluoromethylbenzene (13.7 mL) was photoirradiated with 6 W white LED equipped with neutral density filter of 50% transmittance at room temperature for 3 h under nitrogen atmosphere. The solvent was removed under reduced pressure. The residue was separated by preparative GPC under nitrogen atmosphere to give dimethyl 2-methyl-4-(phenyltellanyl)pentanodioate (64 mg, 12%, a mixture of diastereomers) as yellow oil, together with recovered methyl 2-phenyltellanylpropionate and higher oligomer. ^{1}H NMR (C_6D_6): δ 0.92 (d, J = 7.1 Hz, 3H, CH_3), 0.95 (d, 3H, CH_3), 1.91 (m, 1H, CH_2), 2.16 (m, 1H, CH_2), 2.32 (m, 1H, CH_2), 2.49 (m, 1H, CH_2), 2.60 (m, 2H, CCH), 3.22 (s, 3H, OCH_3), 3.24 (s, 3H, OCH_3), 3.27 (s, 3H, OCH_3), 3.28 (s, 3H, OCH_3), 3.93 (q, J = 7.7 Hz, 1H, CHTe), 3.96 (dd, J = 5.1 Hz, 7.9 Hz, 1H, CHTe), 6.91 (m, 4H, Ph×2), 6.99 (m, 2H, Ph×2), 7.81 (m, 4H, Ph×2). ^{13}C NMR (C_6D_6): δ 16.8, 17.2, 22.5, 23.8, 37.2, 38.0, 39.7, 40.1, 51.1, 51.5, 111.9, 128.9, 129.3, 141.1, 174.6, 175.2, 175.4. HRMS (FAB) *m*/*z*: found 280.0269; calcd for $C_{14}H_{18}O_4Te$ $[M]^+$, 380.0268.

3. Results and Discussion

Structurally well-defined PMA **1a** (M_n = 3200, M_w/M_n = 1.20) bearing a phenyltellanyl group at the ω-end,[4d,5] as dissolved in benzene (0.12 g/mL) and photolyzed at 25 °C with a 500 W Hg lamp through a 390 nm short-wavelength cutoff filter.[6] The complete consumption of **1a** was observed after 4 h in the ^{1}H NMR spectrum as suggested by the quantitative generation of diphenyl ditelluride (Figure 1a). The GPC trace of the products was completely overlapped with that of the starting **1a** (Figure 1b), strongly suggesting the exclusive occurrence of the Disp of PMA end radicals. In the termination of PMA end radicals, the selectivity between Disp and Comb (*D*/*C*) was determined to be 99/1 (Table 1, entry 1).

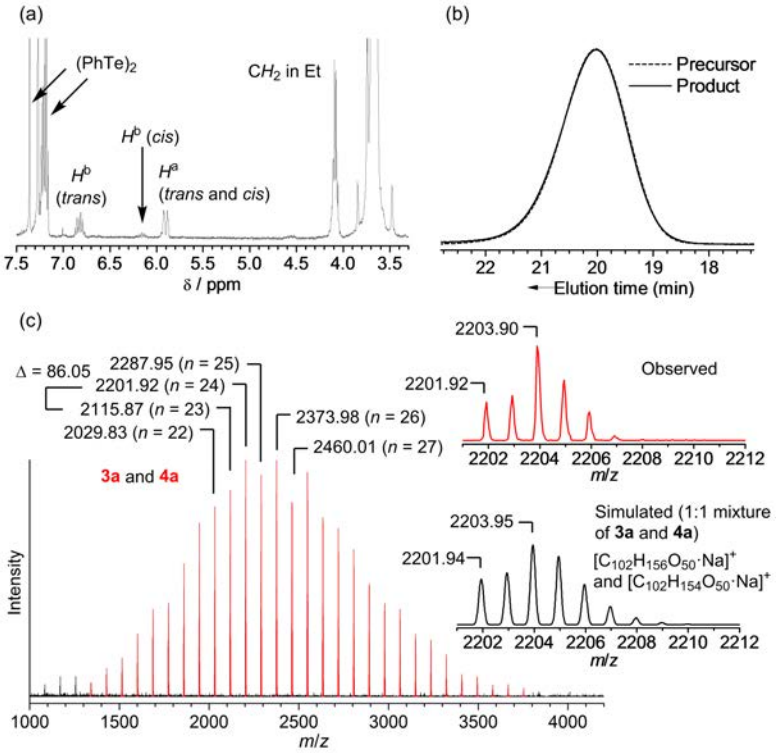

Figure 1. Identification of the termination prodcuts of PMA end radicals. (a) ^{1}H NMR spectrum in C_6D_6. (b) GPC traces. (c) Full (left) and partial (right) MALDI-TOF-MS spectra.

Table 1. Termination reaction of PMA-end radicals. [a),b)]

	Precursor 1a		**Temp.**	**Product**		***D*/*C*** [d)]	k_d/k_c [e)]
	M_n [c)]	M_w/M_n [c)]	(°C)	M_n [c)]	M_w/M_n [c)]		
1	3200	1.20	25	3300	1.20	99/1	99
2	34800	1.16	25	36600	1.15	98/2 [f)]	49 [f)]
3	**6** [g)]	- [h)]	25	- [h)]	- [h)]	100/0 [i)]	>99
4	**7** [j)]	- [h)]	-30[k)]	- [h)]	- [h)]	100/0 [i),l)]	>99
5	3800	1.17	-30	3800	1.16	>99/<1	>99
6	3200	1.20	25	3300	1.19	99/1	99
7	3200	1.20	60	3400	1.23	92/8	12
8	3200	1.20	80	3400	1.21	86/14	6.1
9	3200	1.20	100	3500	1.24	68/32	2.1
10	3200	1.20	120	2500	1.25	52/48	1.1

a) A solution of **1a** was irradiated with a 500 W high pressure Hg lamp through a 390 nm cut-off filter. b) C_6H_6 (entry 1), CH_2Cl_2 (entry 2), C_6D_6 (entry 3), toluene-d_8 (entries 4 and 5), and $PhCF_3$ (entries 6-10) were used as the solvent. c) Determined by GPC calibrated with PMMA standards. d) The ratio of Disp and Comb products of polymer chain end radicals after the correction by the elimination of the effect of mid-chain radicals. e) The ratio of the rates of the Disp and Comb reactions of chain-end radicals calculated from the *D*/*C* ratio. f)

Determined by GPC analysis. g) **6** was used as the precursor. h) Molecular weight was not analyzed by GPC. i) Determined by ^{1}H NMR. j) **7** was used as the precursor. k) The reaction at 25 °C could not be analyzed due to the formation of oligomer derived from MA formed by Disp. l) Methyl propionate and methyl acrylate were obtained as the Disp products.

The occurrence of the exclusive Disp was supported by the structural analysis of the products by matrix-assisted laser desorption/ionization time-of-flight mass spectroscopy (MALDI TOF MS) (Figure 1c) and ^{1}H NMR (Figure 1a). The MS showed a series of monoisotopic molecular ion signals which were separated by a molecular mass of MA (m/z = 86.04). The isotopic distribution of each peak was superimposable to that of the theoretically simulated distribution of a 1:1 mixture of Disp products **3a** and **4a** (Figure 1c, right). On the other hand, the signals corresponding to the Comb product **5a** were not observed at all. The ^{1}H NMR spectrum of the reaction mixture showed characteristic olefinic peaks at 5.90 and 6.82 ppm corresponding to the vinylidene protons of **4a**. The amount of the **4a** was calculated to be 50% from the peak integral of the signals of vinylidene protons and ethyl ester moiety at the polymer α-end, consistent with the exclusive Disp reaction. The selective Disp also occurred in the presence of monomer (100 equiv) in the reaction mixture judged by ^{1}H NMR, while the analysis by GPC was difficult due to the competing propagation.[3] The effect of the molecular weight (chain length) was next examined. When high-molecular-weight PMA **1a** (M_n = 34800, M_w/M_n = 1.16) was photolyzed under the standard conditions employed above, an essentially identical D/C ratio (98/2) was obtained (Table 1, entry 2). The reaction of a low-molecular-weight compound such as a dimer model **6** and a monomer model **7** exclusively gave disproportionation products (D/C = 100/0) (Table 1, entris 3 and 4). The reaction of **7** selevtively gave Disp products (D/C = 100/0). Therefore, these results suggest the very strong tendency of the PMA end radical to undergo Disp.

Temperature significantly influenced the termination mechanism, and not only the Comb products but also products derived from back-biting reactions started to form at high temperature (Table 1, entries 4-8). For example, when the reaction of **1a** was carried out at 60°C, the Comb product **5a** was detected in 4% of the high-molecular-weight region by GPC (Figure S1 in Supporting Information). The structure of Comb product was confirmed by MS analysis (Figure S2). The ^{1}H NMR analysis indicated the formation of Disp product **4a**, as well as a new compound possessing a characteristic olefinic signal (Figure S3). The structure of the new compound was assigned as **8**, which should be formed by the back-biting reaction

of chain-end radical **2a** to form mid-chain radical **9** (and further to **9′**), followed by hydrogen abstraction. The ratio of **4a**/**8** was calculated to be 49/51. Since reactivity of mid-chain radicals, such as **9** (**9'**) would be lower than that of polymer-end radicals due to steric congestion, direct reaction between two mid-chain radicals should be less likely. Therefore, **8** formed most likely by selective hydrogen transfer from mid-chain radical **9** to chain-end radical **2a**. The *D*/*C* ratio between the initially formed, polymer chain-end radical **2a** was determined to be 92/8 under this assumption at 60°C.

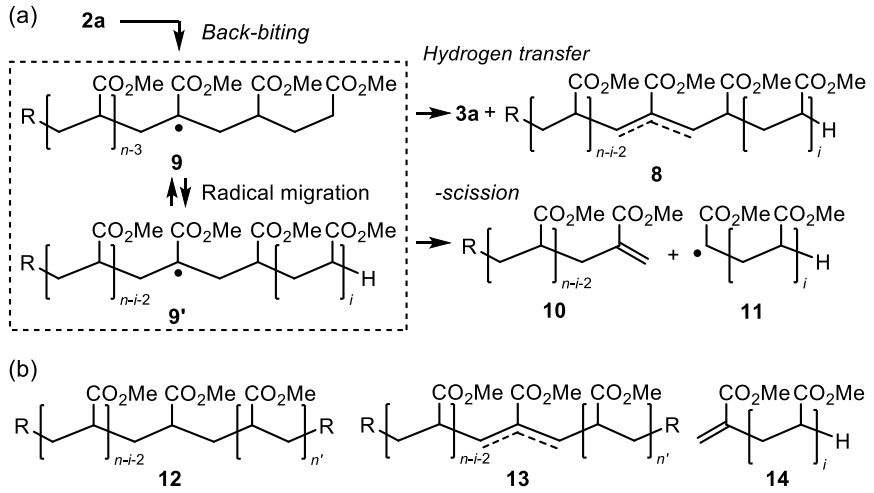

Scheme 2. (a) Back-biting reaction of PMA end radicals, and (b) chemical structure of **12**-**14** formed in a reaction at high temperature. R = $(CH_3)_2(CO_2Et)C$.

The back-biting product **8** further increased at higher temperature (e.g., 83% at 120°C). In addition, the end-vinylidene polymer **10**, which was formed by the β-scission of the mid-chain radical **9** (**9′**) with liberation of radical **11**, was also observed in the MS and ^{1}H NMR analyses, though the amount of end-vinylidene polymer **10** was negligible (<4%) (Figure S2 and S3). The *D*/*C* ratios of the first-formed radical **2a** giving **3a** and **4a** or **5a** were determined to be 86/14, 68/32, and 52/48 at 80, 100 and 120°C, respectively, after the correction for the contribution of back-biting product **8** (Table 2, entries 4–8). The difference in the Gibbs energies of the termination of the first-formed radicals can be obtained as

$$\Delta\Delta G^{\ddagger}_{d/c} = (-46.0 \pm 1.8) - T \times (-117 \pm 5.2) \times 10^{-3} \text{ (kJ mol}^{-1}\text{)}$$

from the Eyring plot (Figure S4). These results also suggest that Disp is highly favored enthalpically and disfavored entropically than Comb is. The same temperature effect is observed for the termination of methyl methacrylate and styrene polymerizations.[3]

Previously, van Herk and coworkers reported that, by pulsed laser polymerization-electron spin resonance analysis, about 70% of the polymer-end radical in the polymerization of butyl acrylate isomerized to the corresponding mid-chain radical by the back-biting reaction at 25°C.[7] In contrast, our result at this temperature was not affected by the back-biting reaction. We attributed the differences to the high concentration of the radical species under our experimental conditions due to its high efficiency in radical generation by the photoirradiation of the organotellurium compounds.[8] Since the termination and back-biting reactions are bimolecular and unimolecular reactions, respectively, the former becomes more prominent when the concentration of the radicals increases. This assumption suggests that the product distribution may change depending on the reaction conditions.

To clarify this point, a control experiment was performed by heating **1a** (M_n = 3200, M_w/M_n = 1.20) in $PhCF_3$ at 120°C in the dark, to slowly generate the PMA end-radical **2a**.[4] The consumption of **1a** was very sluggish and required 12 days. GPC analysis of the reaction mixture showed the formation of a considerable amount of high-molecular-weight polymers and a small amount of low-molecular-weight polymers (Figure S5). The structures of the high-molecular-weight polymers were assigned as dimeric polymer chain **12** and/or **13**, and those of the low-molecular-weight polymers were **10** and **14**, based on MS analysis (Figure S6). All the polymers were derived via the mid-chain radical **9** (**9′**); **10** and **14** formed by β-radical scission from **9** (**9′**), and **12** and **13** should form by the addition of a chain-end radical **2a** to end-vinylidene polymer **10** and subsequent termination reaction. In addition, the ^{1}H NMR analysis indicates that the direct termination reaction of the chain-end radical **2a** was marginal, judging from the almost negligible formation of Disp product **4a** (<6%) (Figure S7). The results clearly indicate that, when the concentration of the polymer-end radical is low, a significant amount of high-molecular-weight polymers are produced from the mid-chain radical **9** (**9'**) formed by the back-biting reaction. In other words, the previous results describing the importance of the Comb reaction were most likely affected by the back-biting and subsequent radical reactions, because there were no molecular-level analyses in the previous reports. Most importantly, these results clearly reveal that the termination mechanism of the first-formed polymer-end radical **2a** involves the exclusive or predominant Disp reaction at ambient temperature.

To explore the generality of the termination mechanism of polyacrylate-end radicals, the experiments were performed for poly(butyl acrylate) (PBA, **1b,** M_n = 5300, M_w/M_n = 1.13) and poly(t-butyl acrylate) (PtBA, **1c**, M_n = 5100, M_w/M_n = 1.10) under the standard condition

used for **1a** at 25 °C. Both for **1b** and **1c**, the GPC trace of the products was completely overlapped with that of the precursor **1b**, revealing the exclusive Disp (Figure S8). The ^{1}H NMR and TOF-MS analysis also supported the formation of Disp products **3b** and **4b**, and **3c** and **4c**, respectively. These results clearly indicated that the termination reaction of polyacrylate end radicals is generally the selective disproportionation.

To help explain the experimental results, *ab initio* molecular dynamics simulations employing the Atom-centered Density Matrix Propagation (ADMP) formalism[9] were carried out at M11/6-31G(d) level of theory.[10] Ten trajectories (singlet multiplicity), based on the density functional theory (DFT) optimized equilibrium structure of triply radical fragment complex **^{3}2a-cpx** (Scheme 3), were propagated for approximately 200 fs at initial nuclear kinetic energies set at 25°C and 120°C. Both sets of results revealed an approximately 50:50 ratio of disproportionation to combination products (Figures S9 and S10). Importantly, and consistent with experiment, the simulations revealed that the textbook combination C_{ipso}–C_{ipso} mechanism does not occur. Instead the combination product is formed through O–C_{ipso} coupling to form a vinyl ether, which is then capable of further reaction to form the disproportionation products (Scheme 3). It was not possible to run the simulations long enough to observe the decomposition of the O–C_{ipso} product, but our calculations indicate that the reaction is strongly thermodynamically favored, and this would explain the experimental product ratios. Indeed, attempts to detect O-C_{ipso} coupling product were unsuccessful in the reaction of **7** or **1a** at -30 °C and analyzed by ^{1}H NMR at the same temperature (Table 1, entries 4 and 5) implying that it is at best a very short-lived intermediate. This novel combination pathway has not previously been considered, and its associated two-step route to the disproportionation products may also help to explain some of the sensitivity of the observed termination products to the reaction.

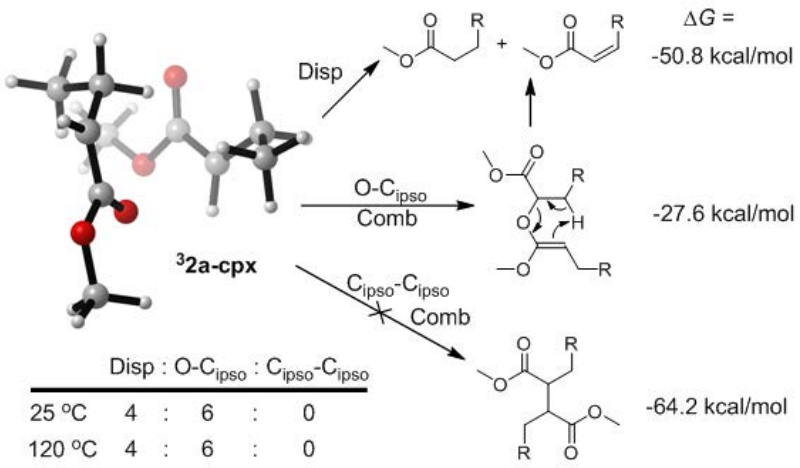

Scheme 3. (a) Termination pathways for model methyl acrylate propagating radicals. The (same) product ratios for the first step were obtained via ADMP simulations at both 25 °C and 120 °C; the relative Gibbs free energies of the overall reactions were obtained via DFT calculations at 25°C (see Supporting Information for further detail).

The unfavorability of the textbook C_{ipso}–C_{ipso} mechanism can be attributed to the distancing of C_{ipso} centers by steric repulsion. In order for combination to occur at the carbon centers, the two overall triply-spin radicals have to approach such that the SOMOs of the two unpaired electrons are orthogonal to each other (see Scheme 4). This orientation allows for effective spin-orbit coupling whereby out-of-plane vibration causes orbital distortions that allow mixing of the triplet and zwitterionic singlet states and intersystem crossing to occur.[11] Once the orbital jump takes place one fragment would be anionic and the other cationic, and combination is possible. In the case acrylate radicals, the carbonyl group of the ester moiety disfavors C_{ipso}–C_{ipso} union by extending the C_{ipso} centers apart. At the same time delocalization of the carbanion electron pair into the C=O π* bond renders the O negatively charged. Combination via O- C_{ipso} is thus realized instead.

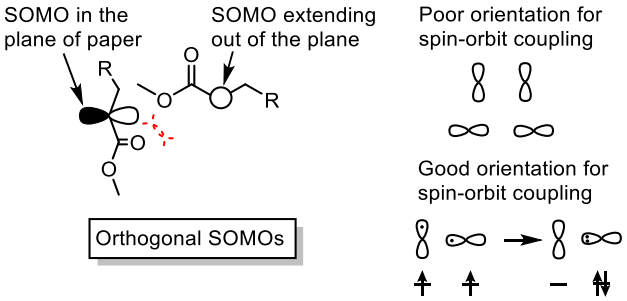

Figure 2. Geometric and orbital requirements effective spin-orbit coupling.

4. Conclusions

In conclusion, the mechanism of the termination of acrylate polymerization, namely bimolecular reaction of polyacrylate end radicals was clearly determined. The mechanism is exclusively or predominantly Disp at ambient temperature, which opposes the current general understanding. The kinetic unfavorability of C_{ipso}-C_{ipso} combination is confirmed via ab initio dynamics simulations, which reveal that instead termination occurs via a mixture of disproportionation and a novel two-step mechanism in O–C_{ispo} which termination is followed

by decomposition to the disproporition products. In addition, this work also clarified the effect of the mid-chain radical generated by the back-biting reaction on the termination mechanism.

Supporting Information

Supporting Information is available from the Wiley Online Library or from the author.

Acknowledgements: This work was partly supported by the Core Research for Evolution Science and Technology of the JST (SY) and by a Grant-in-Aid for Scientific Research from the JSPS (24350057 and 24109005 for SY and 25810021 for YN). MLC gratefully acknowledges generous allocations of supercomputing time on the National Facility of the Australian National Computational Infrastructure and financial support from the Australian Research Council.

Received: Month XX, XXXX; Revised: Month XX, XXXX; Published online:
((For PPP, use "Accepted: Month XX, XXXX" instead of "Published online")); DOI: 10.1002/marc.((insert number)) ((or ppap., mabi., macp., mame., mren., mats.))

Keywords: Radical polymerization, Reaction mechanism, Termination reaction, Molecular dynamics

[1] a) G. Odian, *Principles of polymerization*, John Wiley & Sons, Hoboken, **2004**; b) G. Moad, D. H. Solomon, *The Chemistry of Radical Polymerization*, Elsevier, Amsterdam, **2006**; c) K. Matyjaszewski, T. P. Davis, Wiley-Interscience, New York, **2002**.

[2] a) C. H. Bamford, A. D. Jenkins, *Nature* **1955**, *176*, 78; b) A. K. Chaudhuri, S. R. Palit, *J. Polym. Sci. Part A-1* **1968**, *6*, 2187-2196; c) C. H. Bamford, R. W. Dyson, G. C. Eastmond, *Polymer* **1969**, *10*, 885-899; d) G. Ayrey, M. J. Humphrey, R. C. Poller, *Polymer* **1977**, *18*,

840-843; e) Z. Szablan, T. Junkers, S. P. S. Koo, T. M. Lovestead, T. P. Davis, M. H. Stenzel, C. Barner-Kowollik, *Macromolecules* **2007**, *40*, 6820-6833.

[3] Y. Nakamura, S. Yamago, *Macromolecules*, accepted for publication.

[4] a) S. Yamago, *Chem. Rev.* **2009**, *109*, 5051-5068; b) S. Yamago, K. Iida, J. Yoshida, *J. Am. Chem. Soc.* **2002**, *124*, 2874-2875; c) A. Goto, Y. Kwak, T. Fukuda, S. Yamago, K. Iida, M. Nakajima, J. Yoshida, *J. Am. Chem. Soc.* **2003**, *125*, 8720-8721; d) S. Yamago, Y. Ukai, A. Matsumoto, Y. Nakamura, *J. Am. Chem. Soc.* **2009**, *131*, 2100-2101.

[5] S. Yamago, K. Iida, J. Yoshida, *J. Am. Chem. Soc.* **2002**, *124*, 13666-13667.

[6] a) Y. Nakamura, T. Arima, S. Tomita, S. Yamago, *J. Am. Chem. Soc.* **2012**, *134*, 5536-5539; b) Y. Nakamura, T. Arima, S. Yamago, *Macromolecules* **2014**, *47*, 582-588.

[7] R. X. E. Willemse, A. M. Van Herk, E. Panchenko, T. Junkers, M. Buback, *Macromolecules* **2005**, *38*, 5098-5103.

[8] Y. Nakamura, M. Yu, Y. Ukai, S. Yamago, *ACS Sym. Ser.* **2015**, *1187*, 295-309.

[9] a) S. S. Iyengar, H. B. Schlegel, J. M. Millam, G. A. Voth, G. E. Scuseria, M. J. Frisch, *J. Chem. Phys.* **2001**, *115*, 10291-10302; b) H. B. Schlegel, J. M. Millam, S. S. Iyengar, G. A. Voth, G. E. Scuseria, A. D. Daniels, M. J. Frisch, *J. Chem. Phys.* **2001**, *114*, 9758-9763; c) H. B. Schlegel, S. S. Iyengar, X. Li, J. M. Millam, G. A. Voth, G. E. Scuseria, M. J. Frisch, *J. Chem. Phys.* **2002**, *117*, 8694-8704.

[10] R. Peverati, D. G. Truhlar, *J. Phys. Chem. Lett.* **2011**, *2*. 2810-2817.

[11] N. J. Turro, V. Ramamurthy, J. C. Scaiano, *Modern Molecular Photochemistry of Organic Molecules*, University Science Books, Sausalito, California, 2010.

The termination mechanism of the radical polymerization of acrylate, a long-standing controversy, was unambiguously clarified by the reaction of structurally well-defined polyacrylate end radicals and subsequent product analyses. The exclusive disproportionation was observed at ambient temperature. The two reaction pathways giving the

disproportionation products including a novel stepwise mechanism via O-C_{ipso} coupling are suggested by computational study

Y. Nakamura, R. Lee, M. Coote,* and S. Yamago*

Termination mechanism of the radical polymerization of acrylates

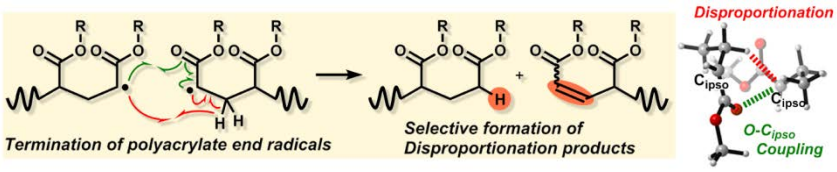

((Supporting Information should be included here for submission only; for publication, please provide Supporting Information as a separate PDF file.))

Supporting Information

for *Macromol. Rapid Commun.*, DOI: 10.1002/marc.2013#####

Termination mechanism of the radical polymerization of acrylates

Yasuyuki Nakamura, Richmond Lee, Michelle Coote,* and Shigeru Yamago*

(1) Supporting Figures

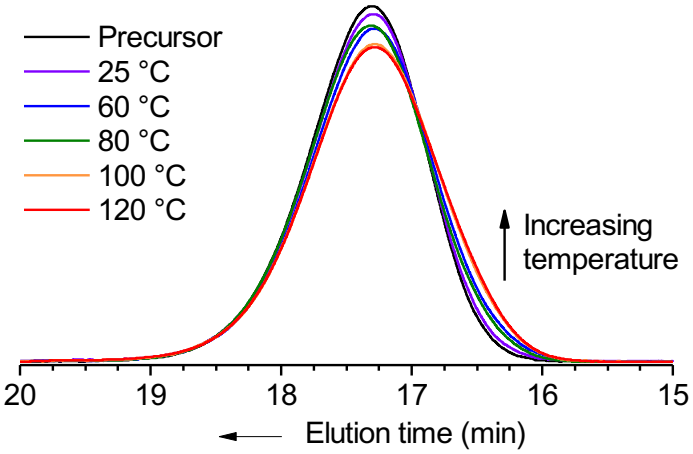

Figure S1. GPC profiles of the termination reaction of PMA end radicals at various temperature. The reactions were carried out by photoirradiation of **1a** (M_n = 3200, M_w/M_n = 1.20) in $PhCF_3$ for 4 h at 25-120 °C (Table 1, entries 6-10). The apparent disproportionation/combination (D/C) ratio determined by GPC peak resolution was 99/1, 96/4, 95/5, 90/10, 88/12 at 25, 60, 80, 100, 120 °C.

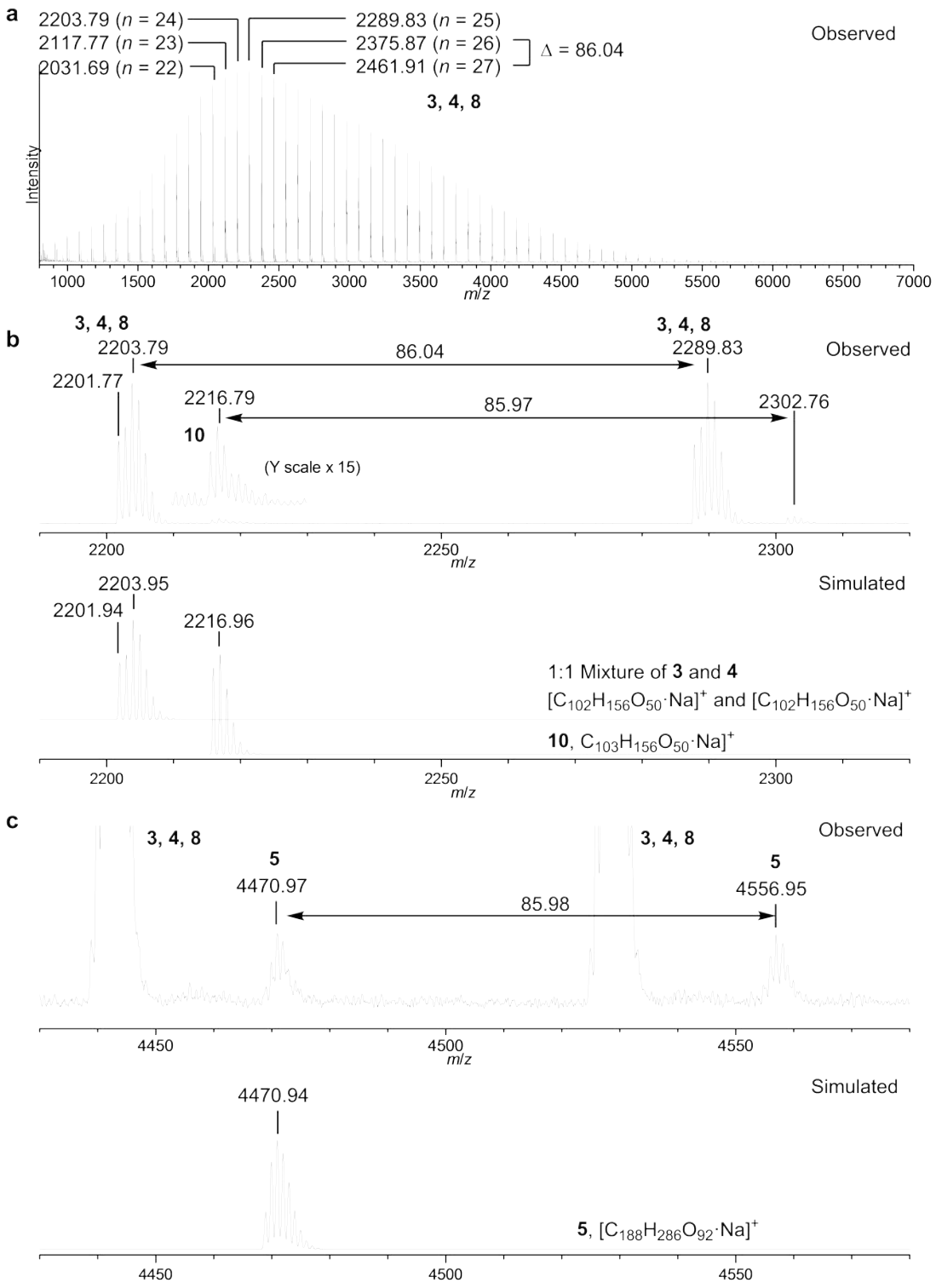

Figure S2. MALDI-TOF-MS spectrum of the product of termination reaction of PMA end radicals at 120 °C. The reactions were carried out by photoirradiation of **1a** (M_n = 3200, M_w/M_n = 1.20) in $PhCF_3$ at 120 °C for 4 h (Table 1, entry 10). **a**, Full spectrum. Because **4a** and **8** have identical molecular weight, they were not distinguished. **b**, Partial spectrum of low molecular weight region with the simulated spectra of 1:1 mixture of **3a** and **4a**, and **10**. **c,** Partial spectrum of high molecular region with the simulated spectra of **5**.

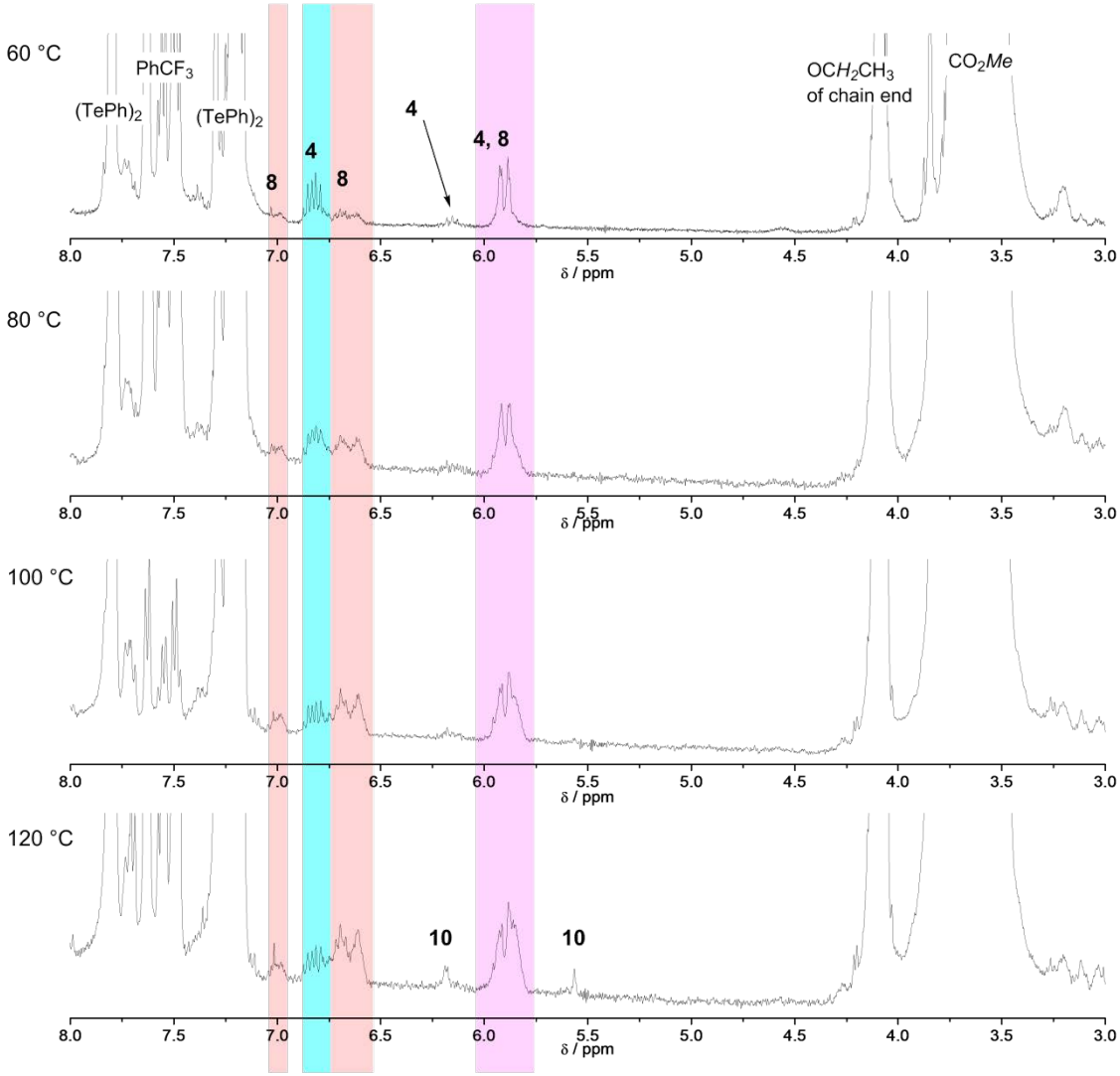

Figure S3. ^{1}H NMR spectra of the product of the termination of PMA end radicals. The reactions were carried out by photoirradiation of **1a** (M_n = 3200, M_w/M_n = 1.20) in $PhCF_3$ for 4 h at 60-120 °C (Table 1, entries 6-10). The broad peaks in the olefinic proton region of 5.7-6 ppm, 6.5-6.7 ppm and 7 ppm were assigned to **8**. From the integral values, the ratio **4a**/**8** was obtained as 49/51, 34/66, 24/76, 15/85 at 60, 80, 100, 120 °C, respectively. In the spectrum at 120 °C, peaks of the vinylic protons of **10** were observed and the amount in termination products was estimated as 4%.

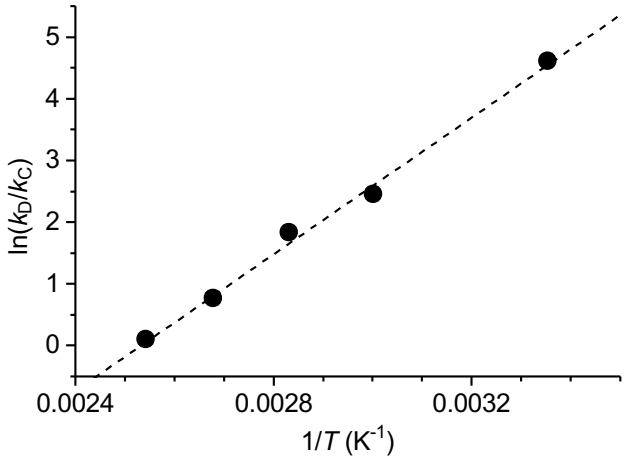

Figure S4. Eyring plot for the disproportionation/combination selectivity of termination reaction of PMA end radical. The selectivity (ln(k_d/k_c), where k_d/k_c is the ratio of the rate of disproportionation and combination) is plotted against inverse absolute temperature (1/T). The reactions were carried out by photoirradiation of **1a** (M_n = 3200, M_w/M_n = 1.20) in $PhCF_3$ for 4 h at 25-120 °C (Table 1, entries 6-10). The difference of Gibbs energy, $\Delta\Delta G^{\ddagger}_{d/c}$, undergoing the disproportionation and the combination was determined as $\Delta\Delta G^{\ddagger}_{d/c} = (-46.0 \pm 1.8) - T \times (-117 \pm 5.2) \times 10^{-3}$ (kJ mol^{-1}).

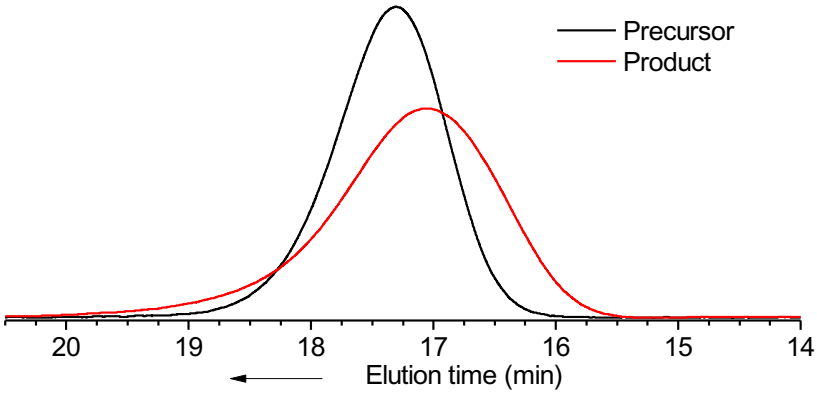

Figure S5. GPC profiles of the termination reaction of PMA end radicals under thermal condition. The reactions were carried out by heating **1a** (M_n = 3200, M_w/M_n = 1.20) in $PhCF_3$ at 120 °C in the dark for 12 days. Peak resolution of the trace of the product showed the ratio of the components of high molecular weight and others was roughly determined as 36:64. The molecular weight of high molecular weight component was nearly twice to that of the precursor.

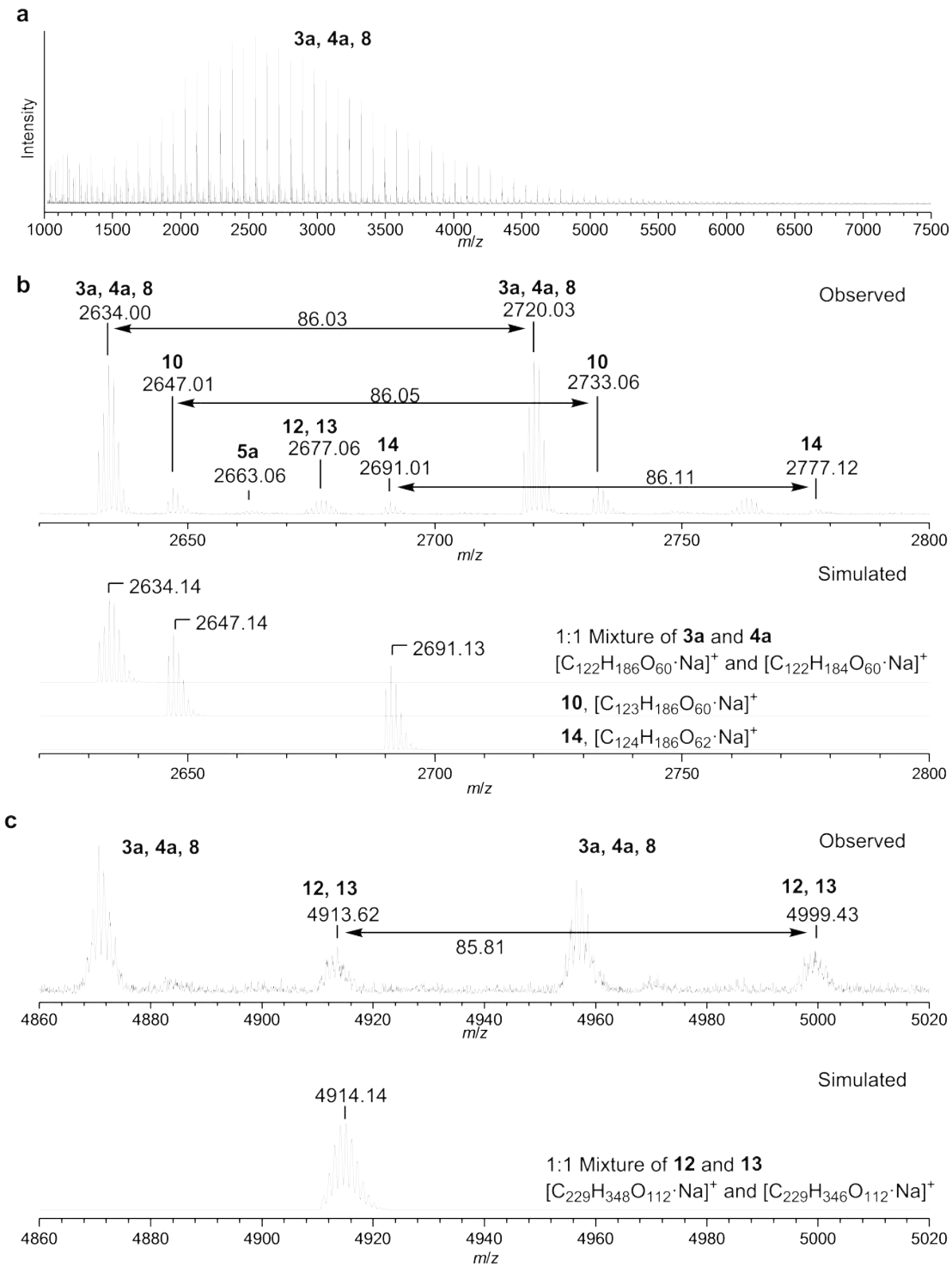

Figure S6. MALDI-TOF-MS spectra of the termination product of PMA end radicals under thermal condition. The reactions were carried out by heating **1a** (M_n = 3200, M_w/M_n = 1.20) in $PhCF_3$ at 120 °C in the dark for 12 days. Molecular ion peak was observed as Na^+ adduct. **a**, Full spectrum. Because **4a** and **8** have identical molecular weight, they were not distinguished. **b**, Partial spectrum with the simulated spectra of 1:1 mixture of **3a** and **4a**, **10** and **14**. **c,** Partial spectrum with the simulated spectra of 1:1 mixture of **12** and **13**.

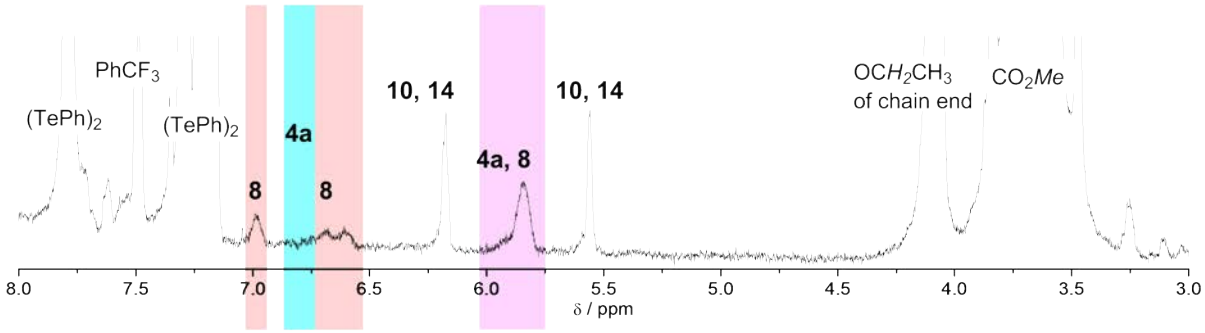

Figure S7. MALDI-TOF-MS spectra of the termination product of PMA end radicals under thermal condition. The reaction were carried out by heating **1a** (M_n = 3200, M_w/M_n = 1.20) in $PhCF_3$ at 120 °C in the dark for 12 days.

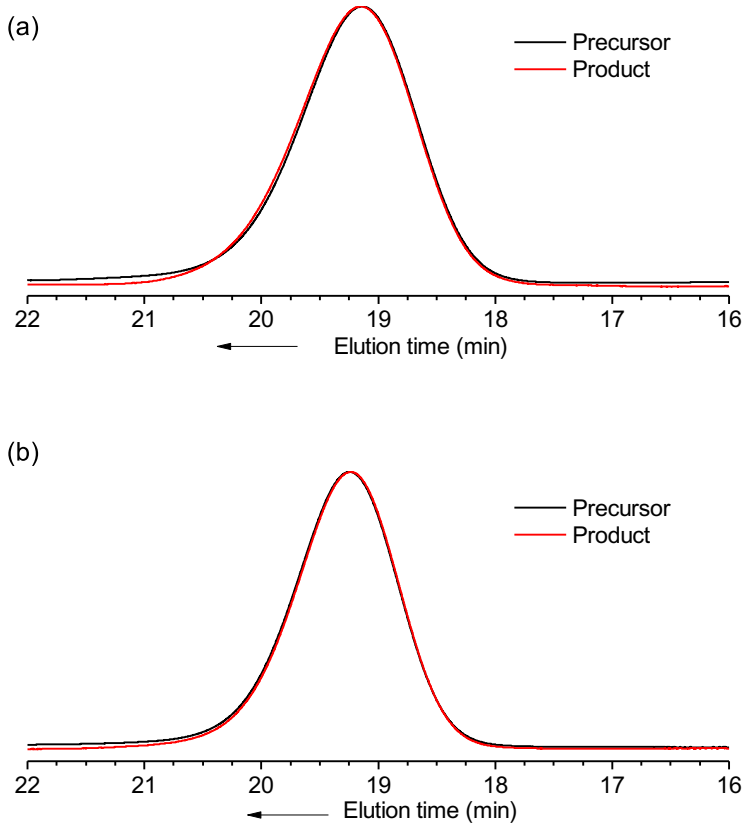

Figure S8. GPC profiles of the termination reaction of (a) PBA and (b) PtBA end radicals. The reactions were carried out by photoirradiation of **1b** (M_n = 5300, M_w/M_n = 1.13) or **1c** (M_n = 5100, M_w/M_n = 1.10) in benzene at 25 °C. *D/C* ratio estimated from GPC traces were >99:<1 or 99:1 for the reactions of **1b** or **1c**, respectively.

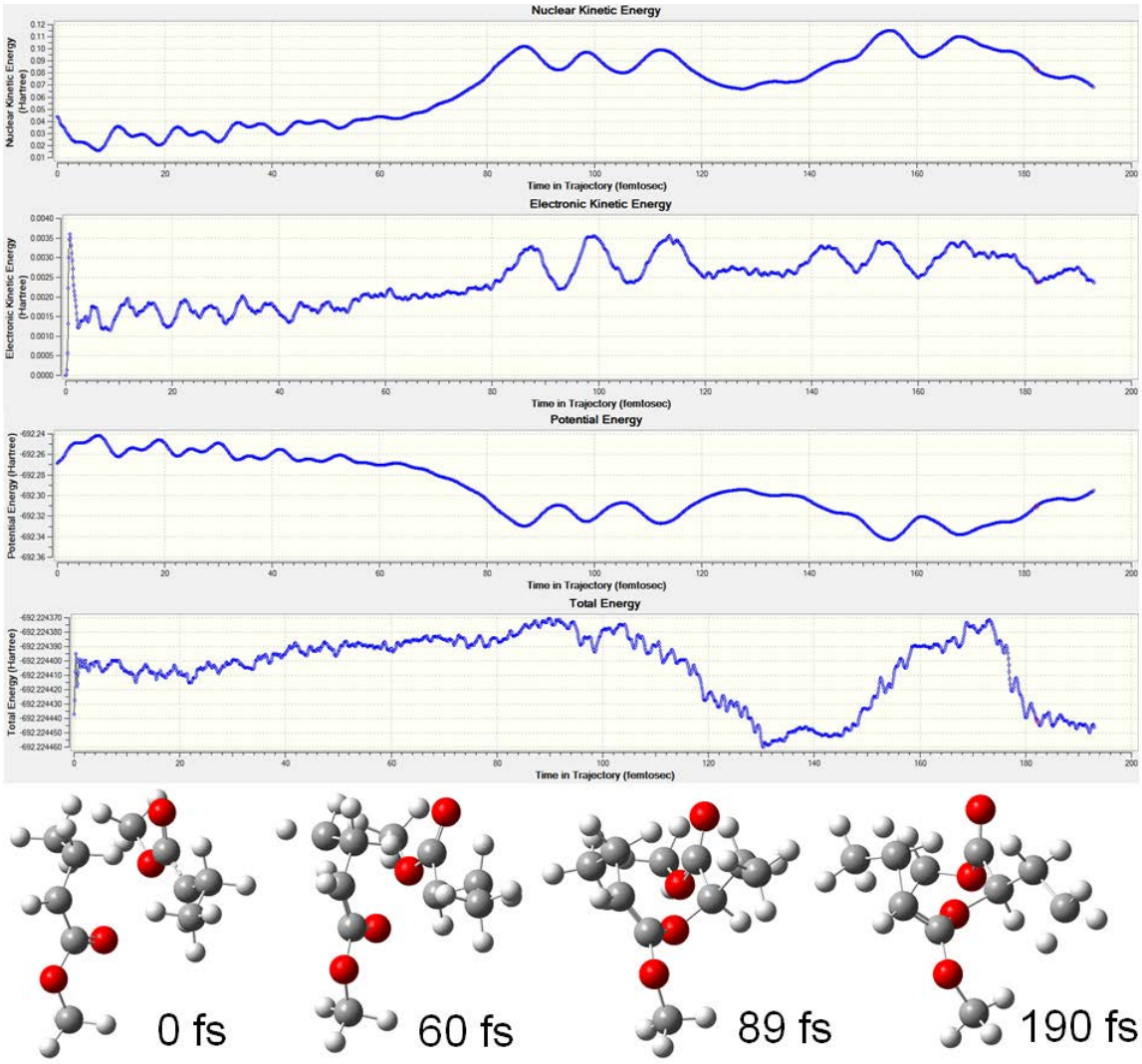

Figure S9. Typical energy profile of the trajectory and snapshots showing O-C_{ipso} combination termination.

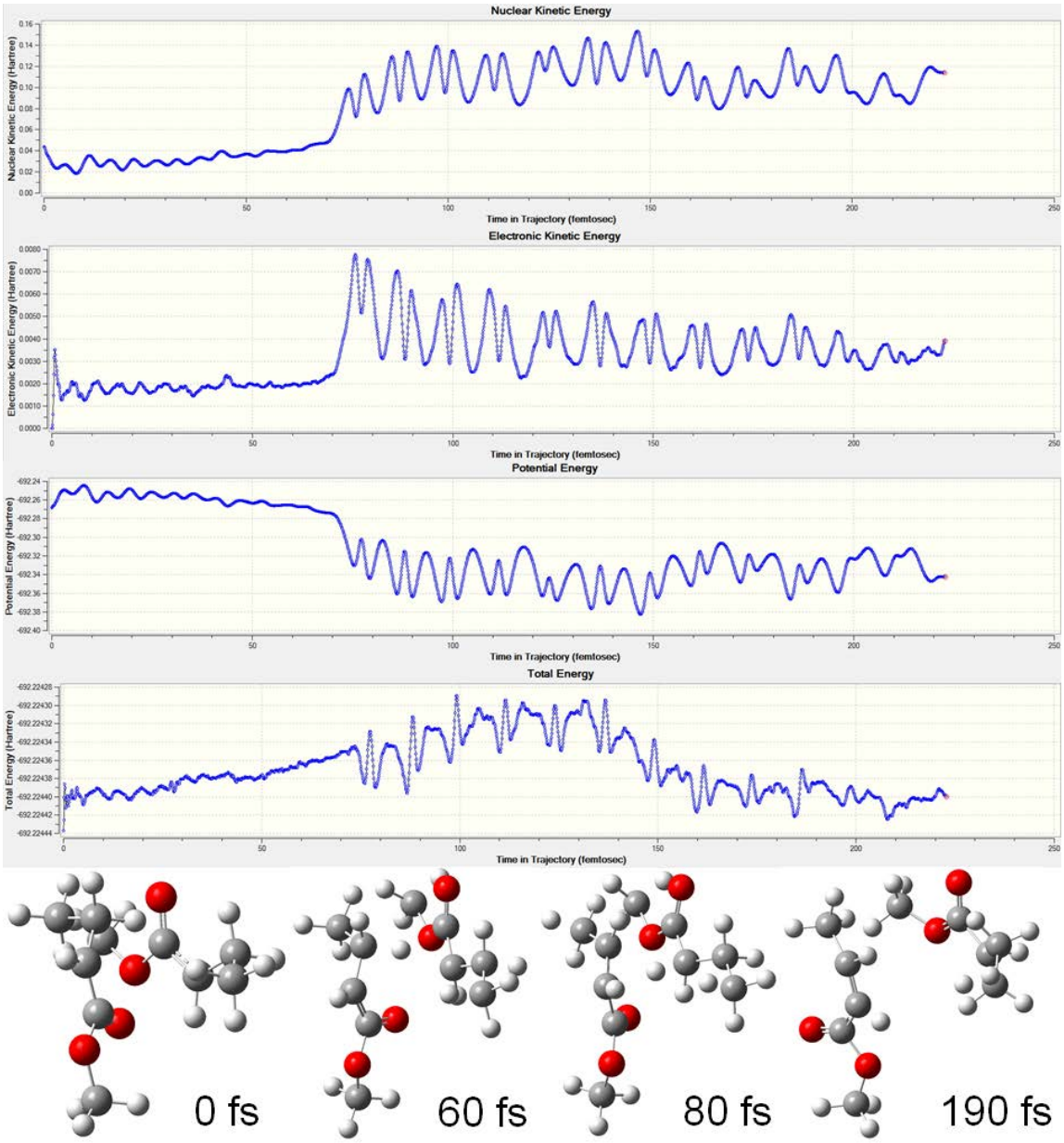

Figure S10. Typical energy profile of the trajectory and snapshots showing disproportionation termination.

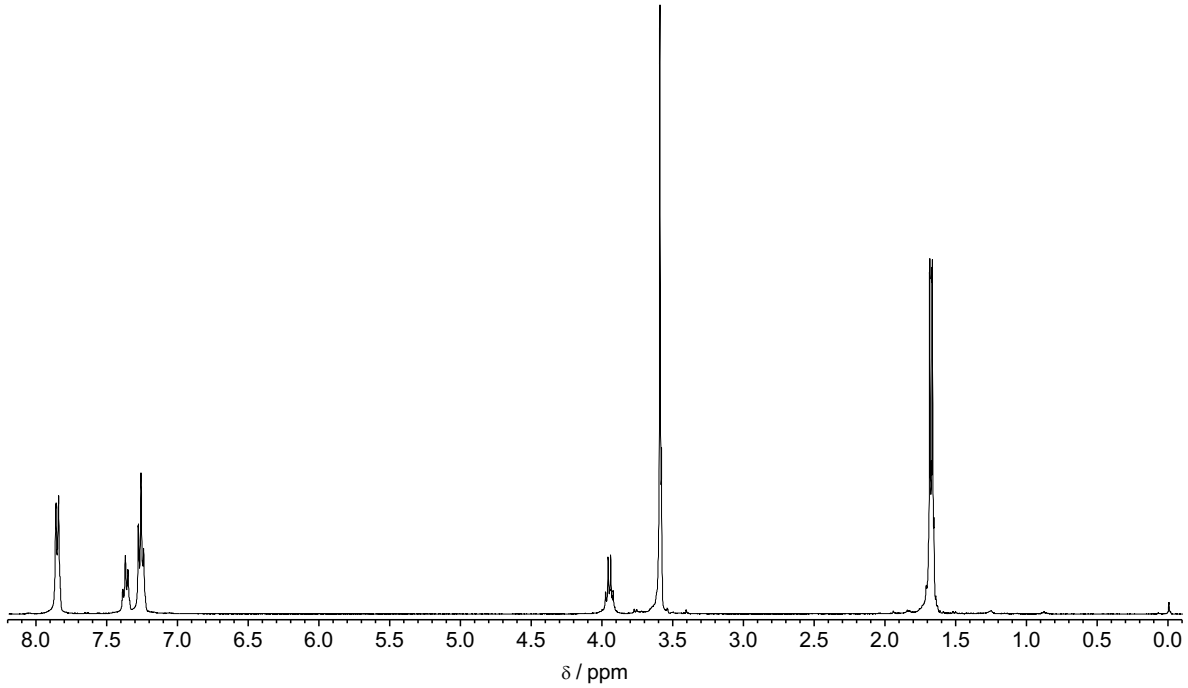

Figure S11. ^{1}H NMR spectrum of 7 in $CDCl_3$.

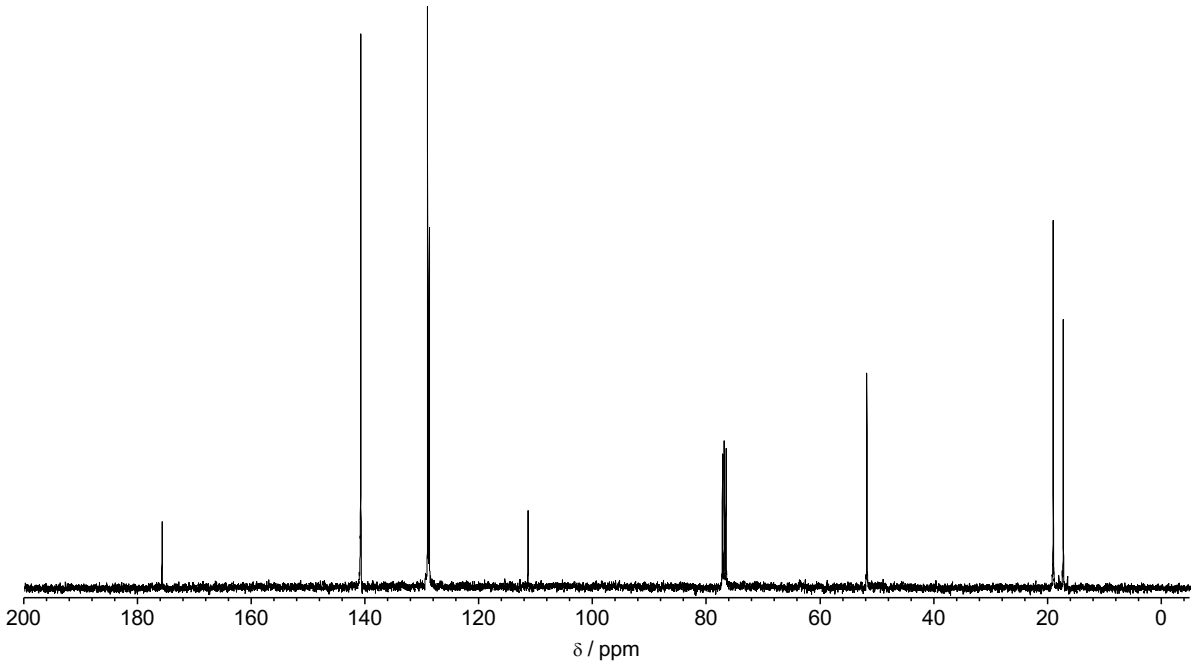

Figure S12. ^{13}C NMR spectrum of 7 in $CDCl_3$.

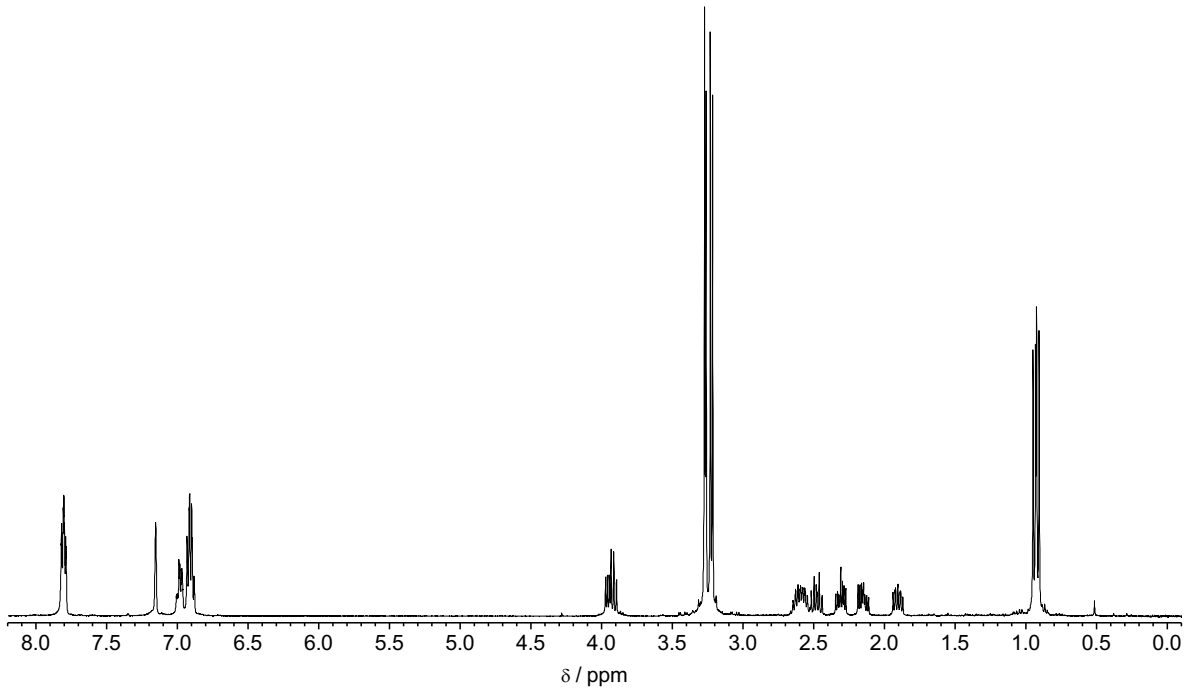

Figure S13. ^{1}H NMR spectrum of 6 in C_6D_6.

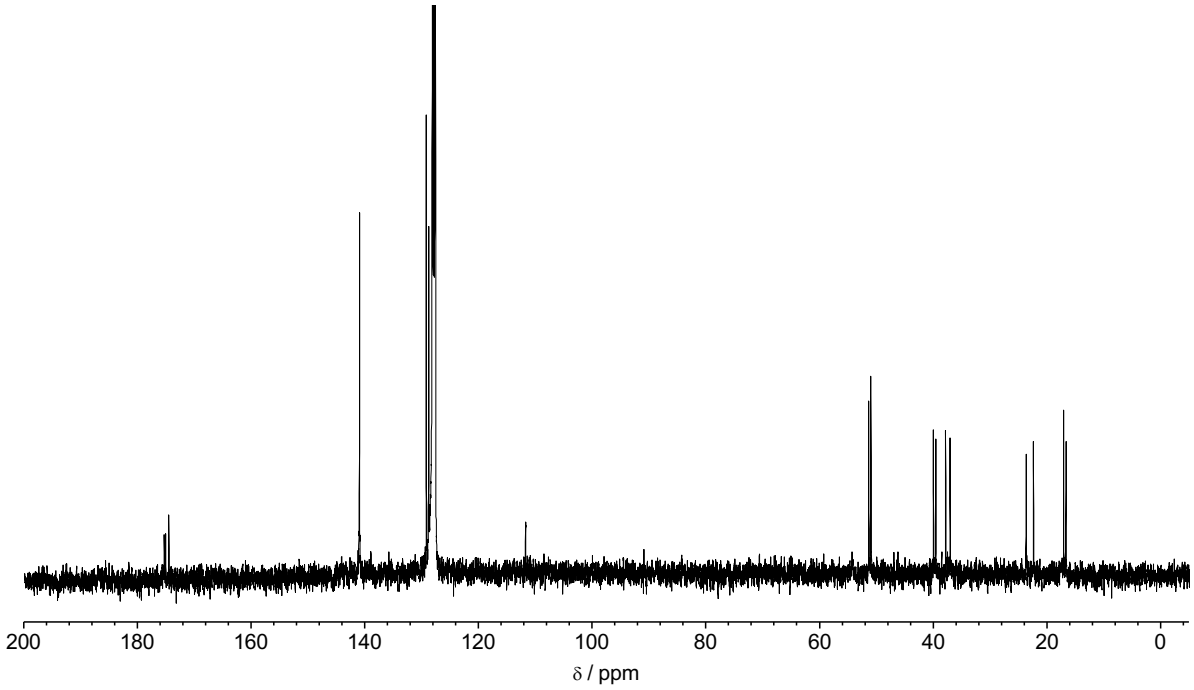

Figure S14. ^{13}C NMR spectrum of 6 in C_6D_6.

(2) Cartesian coordination of calculated structures

^{3}2a-cpx

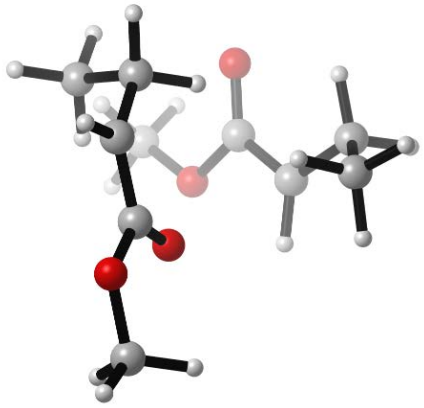

E(M11)= -692.3928171060
Thermal corrections to Gibbs free energy= 0.2192660

C -0.8485334166 2.1476234554 2.3237706613
H -1.4831703797 1.2506234769 2.3609657015
H -1.1800643131 2.7956322424 3.1560478558
C -1.0999503401 2.8611883288 1.0453102115
C 0.6330791258 1.7982788307 2.5341985102
H -0.4461113732 3.6649623727 0.7104098361
C -2.1937621695 2.4822140777 0.1769341519
H 0.7941793647 1.3792838442 3.5359717216
H 1.2662533236 2.6899219445 2.4257408531
H 0.9721486239 1.0624453445 1.7935342675
O -2.9567597471 1.5427741661 0.3709784251
O -2.3059566123 3.2878487929 -0.9048688346
C -3.4003791588 2.9899285412 -1.7732803261
H -4.3485371816 3.0495254753 -1.2230776672
H -3.2956957555 1.9784360658 -2.1872256607
H -3.364509186 3.7387761227 -2.5698503929
H -0.4990440786 -1.4904103041 -0.3309876684
C -0.2883394614 -0.4507973023 -0.6124595092
H -0.5724162868 0.1927072452 0.2356351804
C 1.1605829076 -0.2855181681 -0.9003591367
C -1.1597342877 -0.0414971349 -1.820330754
H 1.8125927663 -1.1274624573 -1.1283450339
C 1.7315767863 1.0461119842 -0.9801292589
H -2.2200527772 -0.1643113451 -1.5653123273
H -0.9777423854 1.01472656 -2.06643131
H -0.9286546049 -0.6543320492 -2.7021213963
O 3.0408358161 1.0410846339 -1.3166411946
O 1.1149150741 2.0811825218 -0.7650273573
C 3.6485627956 2.3333343577 -1.4015833224
H 4.6893512251 2.1578975442 -1.6878329779
H 3.5911823232 2.8419802461 -0.4305207551

H 3.1331533834 2.9448405861 -2.153112493

Disproportionation products

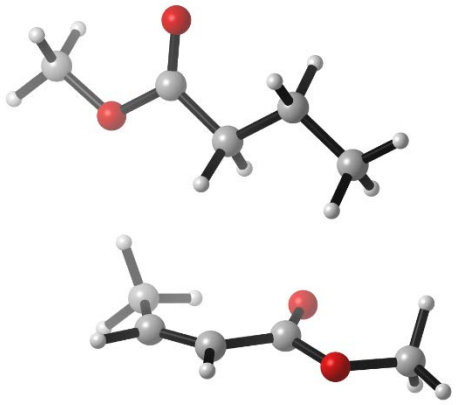

E(M11)= -692.4766763780
Thermal corrections to Gibbs free energy= 0.2221760

C -0.7482302531 2.2978177191 0.2409508807
H -1.1486675303 2.6364625892 1.2074942887
H -1.2638896548 2.8932662859 -0.5253346427
C -1.096123617 0.8247885672 0.0418781486
C 0.7608542944 2.5298354947 0.1699086879
H -0.6814792053 0.4410571095 -0.9052566503
C -2.5860186923 0.5858393436 0.0349985634
H 1.0100764086 3.587670506 0.3277721483
H 1.1497341307 2.2231164688 -0.8116014558
H 1.2902051801 1.9412767231 0.9367270498
O -3.4413881329 1.4420822942 0.0747204165
O -2.8906263526 -0.7288283812 -0.0254552799
C -4.2918797427 -1.0290111267 -0.0520901989
H -4.7599953336 -0.5629092978 -0.9279167522
H -4.7756032627 -0.6470984185 0.8554710112
H -4.3655982865 -2.1190516265 -0.104419087
H 0.466403402 -2.9674691224 1.5529028291
C 0.780492667 -2.3483571584 0.7058176333
H -0.6539417162 0.1943767338 0.8296900868
C 1.7817824075 -1.4913528527 0.9474326209
C 0.0278267007 -2.5720785268 -0.5695406349
H 2.2482914182 -1.4509960675 1.9317407417
C 2.3617528932 -0.5647922304 -0.0539442128
H -0.9981081852 -2.1873667918 -0.4557467987
H 0.4962429766 -2.0741068821 -1.4222633233
H -0.053686521 -3.650843703 -0.7637550534
O 3.4637555591 0.0340621727 0.43901562
O 1.9439288175 -0.3298939349 -1.171717966
C 4.1235464352 0.9417509888 -0.4507145866

H 5.0122374382 1.2903007613 0.0825552736
H 3.4601437922 1.7819630005 -0.6916197143
H 4.399332965 0.4253263623 -1.3785286435

O-Cipso combination product

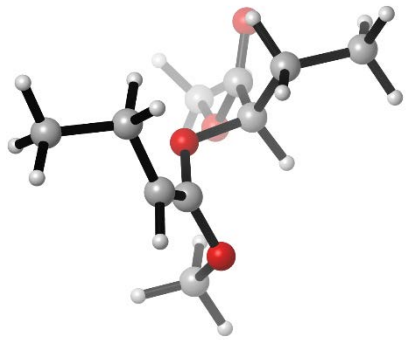

E(M11)= -692.4456356790
Thermal corrections to Gibbs free energy= 0.2280430

C -1.2966748888 1.1152026483 1.3364753577
H -0.3524483933 1.0127083702 1.892990133
H -1.9596054958 0.2935352272 1.6422355332
C -0.9676705016 0.940671108 -0.1391269025
C -1.945652328 2.4690903844 1.6299203329
H -0.4271494012 1.8212247433 -0.5290849429
C -2.2172475891 0.7424714853 -0.9953323716
H -2.1347185626 2.5832636042 2.7047110909
H -2.9064532242 2.5647248703 1.1078248131
H -1.2925537482 3.2967958975 1.3165372017
O -3.3440837721 0.6346669434 -0.5698099408
O -1.9164342418 0.7034527846 -2.2998520156
C -3.0282139919 0.4714716694 -3.1769282694
H -3.7677559603 1.2736953214 -3.0638179168
H -3.4989703021 -0.4888884015 -2.9338732124
H -2.6148915781 0.4593254246 -4.1889514266
H 1.2984182381 -1.4487439317 2.8172227337
C 1.127264009 -1.7591469357 1.7736515535
H 0.0425446379 -1.730269523 1.6028135478
C 1.7984215767 -0.779798017 0.8513873246
C 1.6522946351 -3.188312506 1.580449499
H 2.8773875883 -0.6321319442 0.9227215861
C 1.1648900155 -0.0654796011 -0.0772914739
H 1.1765366241 -3.8847199369 2.2840280154
H 1.450146618 -3.538854322 0.5594662594
H 2.7388345624 -3.2338670244 1.7418073392
O 1.784700138 0.8982330765 -0.8171013778
O -0.1679850596 -0.2316239376 -0.3623665037
C 1.6224280206 0.7513290219 -2.2328644057

H 2.1754309957 1.5771105232 -2.6917387973
H 0.5611464022 0.7992680825 -2.5157050247
H 2.046064977 -0.210405105 -2.5603977395

Cipso -Cipso combination product

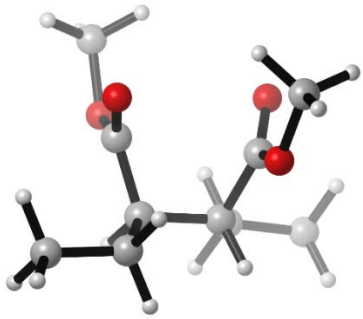

E(M11)= -692.5076403640
Thermal corrections to Gibbs free energy= 0.2317980

C -1.4039784425 1.597144506 1.1009294953
H -1.0945121663 2.1621721364 0.2108636815
H -0.9764937834 2.1077304674 1.9773733647
C -0.7925235655 0.1953827389 1.0267347386
C -2.929627404 1.5655325657 1.2043510989
H -1.1152469391 -0.4097527973 1.8879772808
C -1.2428039039 -0.5189815951 -0.237973282
H -3.3377716857 2.579529554 1.3058122584
H -3.2568576958 0.9834977644 2.0788152525
H -3.3719314212 1.116360121 0.3049925102
O -1.5411879092 0.0429770745 -1.271678313
O -1.1818202584 -1.8510062175 -0.1228581111
C -1.3445179735 -2.5741651272 -1.3533952433
H -0.5496565717 -2.2770557828 -2.0497456913
H -2.3238775569 -2.3520610788 -1.7939773068
H -1.2625278454 -3.6324680717 -1.0914796727
H 0.9361891003 -1.1874282585 2.6531841309
C 1.3805910461 -1.0515710056 1.6553614737
H 1.084707334 -1.9164582032 1.0457122618
C 0.7753233038 0.2117673814 1.0373755578
C 2.9043238772 -0.9772373214 1.7651212426
H 1.085431553 1.1026790323 1.6049941759
C 1.2495917565 0.3862323069 -0.3968946927
H 3.3071949668 -1.8728465478 2.2556776116
H 3.3637038997 -0.9067813151 0.7700111571
H 3.218287755 -0.1025979721 2.3541495525
O 1.1913396928 1.6598763289 -0.8039300274
O 1.5634761949 -0.5291018575 -1.1296987721
C 1.377267488 1.8545868649 -2.2150097406

H 1.2941561166 2.931902147 -2.3817774325
H 0.5934491756 1.3095672071 -2.7568220263
H 2.3633048621 1.4836799548 -2.5195565333

(3) References

[1] E. Kayahara; S. Yamago; Y. Kwak; A. Goto; T. Fukuda *Macromolecules*, **2008**, *41*, 527.
[2] C. Yoshikawa; A. Goto; T. Fukuda *e-Polymers*, **2002**, *13*, 1.
[3] Gaussian 09, Revision D.01, M. J. Frisch, G. W. Trucks, H. B. Schlegel, G. E. Scuseria, M. A. Robb, J. R. Cheeseman, G. Scalmani, V. Barone, B. Mennucci, G. A. Petersson, H. Nakatsuji, M. Caricato, X. Li, H. P. Hratchian, A. F. Izmaylov, J. Bloino, G. Zheng, J. L. Sonnenberg, M. Hada, M. Ehara, K. Toyota, R. Fukuda, J. Hasegawa, M. Ishida, T. Nakajima, Y. Honda, O. Kitao, H. Nakai, T. Vreven, J. Montgomery, J. A. , J. E. Peralta, F. Ogliaro, M. Bearpark, J. J. Heyd, E. Brothers, K. N. Kudin, V. N. Staroverov, R. Kobayashi, J. Normand, K. Raghavachari, A. Rendell, J. C. Burant, S. S. Iyengar, J. Tomasi, M. Cossi, N. Rega, J. M. Millam, M. Klene, J. E. Knox, J. B. Cross, V. Bakken, C. Adamo, J. Jaramillo, R. Gomperts, R. E. Stratmann, O. Yazyev, A. J. Austin, R. Cammi, C. Pomelli, J. W. Ochterski, R. L. Martin, K. Morokuma, V. G. Zakrzewski, G. A. Voth, P. Salvador, J. J. Dannenberg, S. Dapprich, A. D. Daniels, Ö. Farkas, J. B. Foresman, J. V. Ortiz, J. Cioslowski and D. J. Fox, Gaussian Inc., Wallingford CT, 2013.
[4] S. S. Iyengar, H. B. Schlegel, J. M. Millam, G. A. Voth, G. E. Scuseria and M. J. Frisch, *J. Chem. Phys.*, **2001**, *115*, 10291-10302.
[5] H. B. Schlegel, J. M. Millam, S. S. Iyengar, G. A. Voth, G. E. Scuseria, A. D. Daniels and M. J. Frisch, *J. Chem. Phys.*, **2001**, *114*, 9758-9763.
[6] H. B. Schlegel, S. S. Iyengar, X. Li, J. M. Millam, G. A. Voth, G. E. Scuseria and M. J. Frisch, *J. Chem. Phys.*, **2002**, *117*, 8694-8704.
[7] R. Peverati and D. G. Truhlar, *J. Phys. Chem. Lett.,* **2011**, *2*, 2810-2817.
[8] R. Ditchfield, W. J. Hehre and J. A. Pople, *J. Chem. Phys.*, **1971**, *54*, 724-728.
[9] W. J. Hehre, R. Ditchfield and J. A. Pople, *J. Chem. Phys.*, **1972**, *56*, 2257-2261.